Journal of Physiology (1993), **469**, *pp.* 693–716
With 12 figures
Printed in Great Britain

CHARACTERIZATION OF Ca^{2+} SIGNALS INDUCED IN HIPPOCAMPAL CA1 NEURONES BY THE SYNAPTIC ACTIVATION OF NMDA RECEPTORS

BY SIMON ALFORD*‡§, BRUNO G. FRENGUELLI‡, J. GEORGE SCHOFIELD† AND GRAHAM L. COLLINGRIDGE*‡‖

*From the *Department of Pharmacology and the †Department of Biochemistry, School of Medical Sciences, University of Bristol, Bristol BS8 1TD and ‡Department of Pharmacology, The Medical School, The University of Birmingham, Edgbaston, Birmingham B15 2TT*

(*Received 19 May 1992*)

SUMMARY

1. A combination of confocal microscopy, whole-cell patch-clamp recording, intracellular dialysis and pharmacological techniques have been employed to study Ca^{2+} signalling in CA1 pyramidal neurones, within rat hippocampal slices.

2. In the soma of CA1 neurones, depolarizing steps applied through the patch-pipette resulted in transient increases in the fluorescence emitted by the Ca^{2+} indicator fluo-3. The intensity of the fluorescence transients was proportional to the magnitude of the Ca^{2+} currents recorded through the pipette. Both the somatic fluorescence transients and the voltage-activated Ca^{2+} currents ran down in parallel over a period of between approximately 15–45 min. The fluorescence transients were considered, therefore, to be caused by increases in cytosolic free Ca^{2+}.

3. Under current-clamp conditions, high-frequency (tetanic) stimulation (100 Hz, 1 s) of the Schaffer collateral–commissural pathway led to compound excitatory postsynaptic potentials (EPSPs) and somatic Ca^{2+} transients. The somatic Ca^{2+} transients were sensitive to the *N*-methyl-D-aspartate (NMDA) receptor antagonist D-2-amino-5-phosphonopentanoate (AP5; 100 μM). These transients, but not the EPSPs, disappeared with a time course similar to that of the run-down of voltage-gated Ca^{2+} currents. Tetanus-induced somatic Ca^{2+} transients could not be elicited under voltage-clamp conditions.

4. Fluorescence images were obtained from the dendrites of CA1 pyramidal neurones starting at least 30 min after obtaining whole-cell access to the neurone. Measurements were obtained only after voltage-gated Ca^{2+} channel activity had run down completely.

5. Tetanic stimulation of the Schaffer collateral–commissural pathway resulted in compound EPSPs and excitatory postsynaptic currents (EPSCs), under current- and voltage-clamp, respectively. In both cases, these were invariably associated with

§ Present address: Department of Physiology, Northwestern University Medical School, 303 E. Chicago Avenue, Chicago, IL 60611–3008, USA.

‖ To whom correspondence should be addressed.

dendritic Ca^{2+} transients. In cells voltage-clamped at −35 mV, the fluorescent signal increased on average 2-fold during the tetanus and decayed to baseline values with a half-time ($t_{\frac{1}{2}}$) of approximately 5 s.

6. The α-amino-3-hydroxy-5-methyl-4-isoxazolepropionate (AMPA) receptor antagonist, 6-cyano-7-nitroquinoxaline-2,3-dione (CNQX; 10 μM) partially reduced the tetanus-induced EPSC without affecting the Ca^{2+} transients. In contrast, AP5, which also depressed the EPSC, substantially reduced or eliminated the Ca^{2+} transients.

7. In normal (i.e. 1 mM Mg^{2+}-containing) medium, NMDA receptor-mediated synaptic currents displayed the typical region of negative slope conductance in the peak *I–V* relationship (between −90 and −35 mV). The dendritic tetanus-induced Ca^{2+} transients also displayed a similar anomalous voltage dependence, decreasing in size from −35 to −90 mV.

8. In slices perfused for at least 1 h with medium which was nominally free of Mg^{2+}, the voltage dependence of the dendritic tetanus-induced Ca^{2+} transients and EPSCs was linear. At membrane potentials slightly more positive than 0 mV, small dendritic tetanus-induced Ca^{2+} transients, associated with outward synaptic currents, were recorded.

9. The L-type Ca^{2+} channel antagonist nitrendipine (10 μM) reversibly abolished the voltage-gated Ca^{2+} currents evoked within minutes of obtaining whole-cell access, by voltage steps between −35 and 0 mV. It had no effect, however, on tetanus-induced dendritic Ca^{2+} transients, evoked from −35 mV (or −70 mV).

10. Analysis of small (*circa* 4 μm) lengths of dendrite revealed oscillations in the decaying phase of the tetanus-induced Ca^{2+} transients, particularly where the decay phase was relatively slow ($t_{\frac{1}{2}} > 5$ s). Neighbouring small segments displayed markedly heterogeneous behaviour, indicating the independence of Ca^{2+} signalling within these regions. The oscillations were substantially reduced by AP5 (100 μM).

11. Ryanodine (10 μM) or thapsigargin (10 μM), which interfere with the release of Ca^{2+} from intracellular stores, reduced the peak tetanus-induced Ca^{2+} transient by approximately 65%.

12. Analysis within spine-like structures also revealed Ca^{2+} transients. The Ca^{2+} transients within 'spines' decayed rapidly. Sustained Ca^{2+} elevations were not seen.

13. We conclude that tetanic stimulation of the Schaffer collateral–commissural pathway, through the synaptic activation of NMDA receptors, elevates Ca^{2+} by at least three mechanisms. There is entry into the soma through voltage-gated Ca^{2+} channels, entry into the dendrites by permeation through NMDA receptor-operated channels and release from intracellular stores. The significance of these distinct Ca^{2+} signals for synaptic plasticity is discussed.

INTRODUCTION

The entry of Ca^{2+} into neurones is involved in a variety of physiological and pathological conditions, including synaptic plasticity and neuronal injury and death. There is particular interest in Ca^{2+} entry following the activation of NMDA receptors since NMDA receptor antagonists (Collingridge, Kehl & McLennan, 1983; Bliss & Collingridge, 1993) and Ca^{2+} chelators (Lynch, Larson, Kelso, Barrionuevo & Schottler, 1983; Malenka, Kauer, Perkel & Nicoll, 1989) can, under many circumstances, prevent the induction of the form of synaptic plasticity known as

long-term potentiation (LTP). Furthermore, NMDA receptor antagonists are anti-epileptogenic and offer neuroprotection against, for example, ischaemic cell death (Croucher, Collins & Meldrum, 1982; Simon, Swan, Griffiths & Meldrum, 1984).

In the hippocampus, a region which is richly endowed with NMDA receptors (Monaghan & Cotman, 1986), high-frequency (i.e. tetanic) stimulation of afferent pathways elevates Ca^{2+} in the dendrites of pyramidal neurones, as assessed using the Ca^{2+} indicator fura-2 (Regehr & Tank, 1990, 1992; Müller & Connor, 1991). This effect involves, in part, the synaptic activation of NMDA receptors, since the specific NMDA receptor antagonist D-2-amino-5-phosphonopentanoate (AP5) (Davies, Francis, Jones & Watkins, 1981) reduces the Ca^{2+} signal. However, the NMDA receptor-dependent Ca^{2+} signal will be a composite response comprising Ca^{2+} permeating NMDA receptor-operated channels (hereafter referred to as NMDA channels) and Ca^{2+} entering through voltage-gated Ca^{2+} channels, activated by the NMDA receptor-mediated depolarization (Mayer, MacDermott, Westbrook, Smith & Barker, 1987). Furthermore, this signal may also involve a magnification factor provided by Ca^{2+} release from intracellular stores (Tsien & Tsien, 1990). Since the Ca^{2+} signals provided by these different pathways are likely to have distinct functions within neurones, it is important to separate the Ca^{2+} signal into its component parts.

In the present study we have combined confocal microscopy with whole-cell patch-clamp recording, intracellular perfusion and pharmacological approaches to identify three distinct components to the Ca^{2+} signal initiated by the synaptic activation of NMDA receptors in rat hippocampal slices. Some of this work has appeared in abstract form (Alford & Collingridge, 1990*a*, *b*; Alford, Schofield & Collingridge, 1991; Alford, Frenguelli & Collingridge, 1992).

METHODS

The experimental arrangement is shown schematically in Fig. 1. Hippocampal slices (200 μm) were prepared, using a vibroslice, from 11–17-day-old, halothane-anaesthetized rats. The slices were mounted on glass coverslips where they were continuously superfused at approximately 1 ml min^{-1} with medium of the following composition (mM): NaCl, 124; $NaHCO_3$, 26; KCl, 3; NaH_2PO_4, 1·25; $CaCl_2$, 2; $MgSO_4$, 1; D-glucose, 10; picrotoxin, 0·05 (bubbled with 95% O_2–5% CO_2) at room temperature. Whole-cell patch-clamp recordings (seal resistances > 5 GΩ) were obtained from neurones located approximately 30–50 μm from the coverslip, using a 'blind' method (Blanton, Loturco & Kreigstein, 1989). The electrodes contained, unless otherwise noted (mM): $CsMeSO_4$, 130; NaCl, 1; $MgCl_2$, 1; QX-314 (*N*-(2,6-dimethyl-phenylcarbamoylmethyl)-triethylammonium bromide), 5; EGTA, 0·1 or 0·05; Hepes, 5 (adjusted to pH 7·3). Series resistances, measured at various times throughout the experiment, varied between 10 and 20 MΩ and were not compensated. After obtaining a stable whole-cell recording, approximately 4 μl of patch solution containing 50 μM fluo-3, free acid (Tsien, 1988) was added to the pipette using a patch-perfusion system. This comprised a length of silica tubing (outer diameter, 170 μm), flame-pulled to a fine tip and positioned to within 100 μm of the tip of the patch pipette. The silica tubing was led through a separate port in the pipette holder and was connected to a Hamilton syringe. The free Ca^{2+} concentration in this electrode solution (measured in a cuvette using conventional fluorimetry) was 15 nM.

Images were obtained using a laser-scanning confocal microscope (BioRad MRC 500 or MRC 600; Fine, Amos, Durbin & McNaughton, 1988), connected to an inverted microscope (Nikon Diaphot, Japan) fitted with a 20 × 0·75 NA objective. Excitation was achieved using an Argon ion laser (wavelength (λ) = 488 nm) and fluorescence measured at λ > 515 nm. Optical sections (3 μm from peak to 50% intensity) of selected areas (defined by 96 × 128 pixels) were obtained at 500 ms

intervals. Up to thirty-two successive frames were obtained for each tetanus and up to eight tetani were applied to each cell. With this protocol, bleaching of the dye during the course of an experimental run was typically less than 10%; time spent under illumination was kept to a minimum and presumably the dye contained within the small illuminated region was continuously replenished from the large reservoir of dye in the remainder of the cell/pipette. For each optical

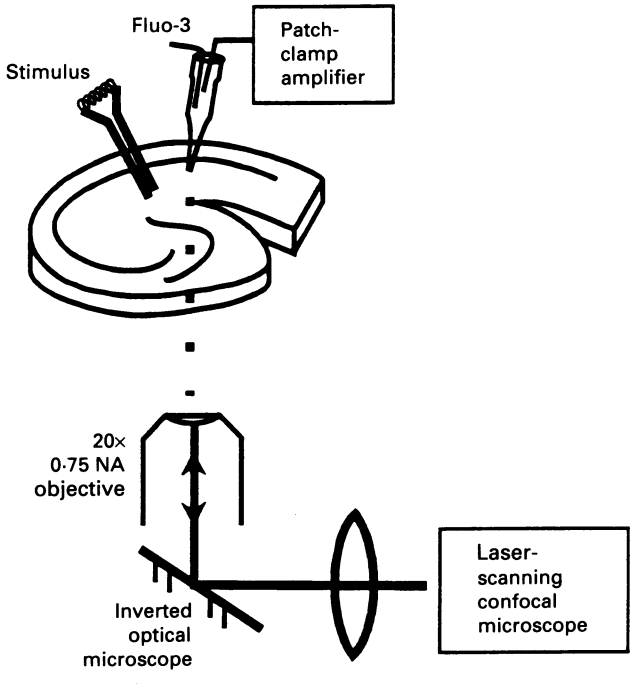

Fig. 1. Experimental arrangement.

section obtained during an experiment the photomultiplier gain was adjusted to optimize the dynamic range without incurring saturation at the peak intensity. Optical sections from the soma were obtained within a few minutes of dye application. To obtain adequate fluorescence from the dendrites it was necessary to wait for at least 30 min. Although the spatial resolution of our system is approximately 1 μm and enables us to detect spine-like structures, we chose, for most experiments, to integrate over a length of dendrite to increase the accuracy of the measurements. The dendritic segments will consist of the average signal provided by many spines and the underlying dendritic branches. To obtain the measurement we subtracted the background signal on a frame-by-frame basis and expressed each image as a percentage of the average of the 3–4 pre-stimulus images. The background was calculated from a region of the slice adjacent to the fluo-3-loaded neurone at the beginning and end of each experimental run. Sometimes there was a small reduction (typically less than 10%) in the fluorescence in these two frames; in these cases a ramp was constructed between these two values and the corresponding background calculated for each frame.

The Schaffer collateral–commissural pathway was stimulated, within 500 μm of the cell, in stratum radiatum (close to the cell body layer) to stimulate fibres impinging upon the apical dendrites approximately 50–150 μm from the soma. Single shocks were delivered at 15 s intervals and tetanic stimulation was delivered at 100 Hz for 1 s (at test intensity) via a bipolar stimulating electrode with an approximate diameter of 100 μm. Despite the pharmacological blockade of synaptic inhibition, after-discharges were not seen due to the thin nature of the slices which precluded a direct connection between areas CA3 and CA1.

To obtain sufficient dendritic resolution it was necessary to maintain stable whole-cell recordings for a minimum period of 30 min from neurones located approximately 50 μm from the bottom surface of the slice. Sometimes upon dye filling, the primary dendrites were found to penetrate deeper into the slice, thereby compromising the image quality. These neurones were discarded. The input resistance, holding current or membrane potential and the synaptic responses, evoked by single-shock stimulation, were monitored for each neurone throughout each experiment. If there was any deterioration in any of these parameters the experiment was terminated. These strict neuronal selection criteria precluded the obtainment of large values of n. However, each major point was addressed using more than one experimental protocol. Data are presented as means $\pm$ S.E.M.

RESULTS

Experiments were performed on fifty neurones which had resting membrane potentials, upon obtaining whole-cell access, of -58 ± 4 mV and input resistances of 205 ± 55 MΩ (calculated from a sample of forty-two neurones). Low-frequency stimulation of the Schaffer collateral–commissural pathway always elicited an inward synaptic current which was often curtailed and followed by an outward current. The outward current was routinely eliminated by the addition of picrotoxin to the perfusate and the inclusion of Cs^+ and QX-314 in the patch solution.

Ca^{2+} entry through voltage-gated Ca^{2+} channels

Shortly after the injection of fluo-3 into the electrode tip, voltage steps sufficient to evoke voltage-gated Ca^{2+} currents, were applied to the neurone and the slice was scanned at low resolution to locate its position. In each case, its location was revealed by fluorescence transients which appeared in response to the voltage steps.

The somatic fluorescence transients were proportional to the size of the Ca^{2+} currents evoked (Fig. 2). With repetitive voltage steps both parameters decreased in parallel (not illustrated). In addition, since no ATP support was provided, the Ca^{2+} currents (and somatic fluorescence transients) decreased with time and eventually disappeared (Fig. 2*A*). The time for run-down of Ca^{2+} currents varied between cells but usually took between 15 and 45 min after obtaining whole-cell access. The use of ATP-deficient solutions was deliberate since it removed any complications arising from voltage breakthrough associated with synaptic responses leading to Ca^{2+} entry through voltage-gated Ca^{2+} channels in the dendrites of these neurones. However, the role of somatic voltage-dependent conductances in providing a Ca^{2+} signal in response to synaptic activation could be studied shortly after obtaining whole-cell access.

Tetanic stimulation elicited a somatic Ca^{2+} transient in eight neurones recorded under current-clamp conditions (Fig. 3*A*). In each of the six cells tested, the Ca^{2+} transient was absent when the same tetanus was delivered under voltage-clamp conditions, at either -70 or -35 mV (Fig. 3*B*). The tetanus-induced somatic Ca^{2+} transients, recorded under current-clamp conditions, were reduced by AP5 in four of five cells tested (by at least 33%; Fig. 3*A*). This indicates that, as would be expected, dendritic NMDA receptor-mediated EPSPs can contribute to the depolarization which activates somatic voltage-gated Ca^{2+} channels.

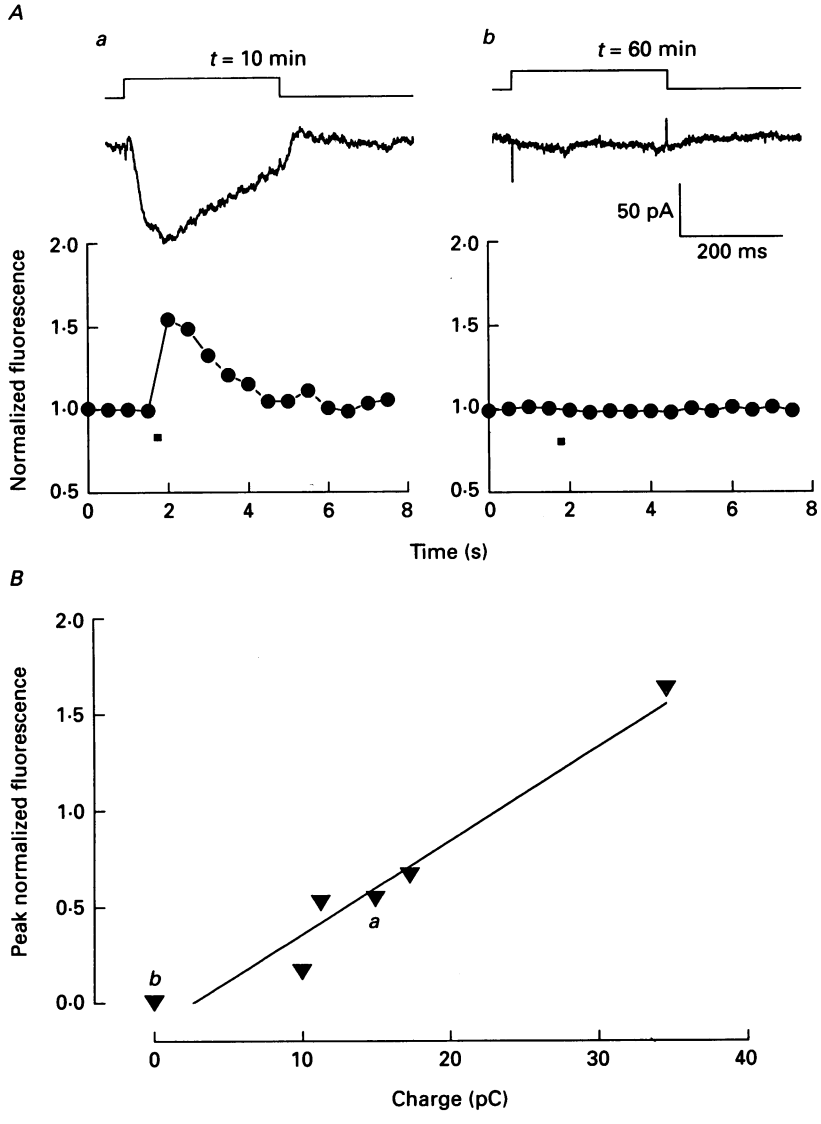

Fig. 2. Activation of voltage-gated Ca^{2+} currents is associated with a rise in somatic fluorescence. *A*, run-down of voltage-gated Ca^{2+} currents and the associated fluorescence signals: *a*, shows the leak-subtracted voltage-gated currents and the associated change in fluorescence induced by a 250 ms voltage-step from −60 to −20 mV recorded 10 min after obtaining whole-cell access; *b*, shows the absence of voltage-gated currents and fluorescence changes induced by an identical step 60 min after obtaining whole-cell access. *B*, shows the relationship between the charge entering the cell and the increase in fluorescence in response to voltage steps. Different sized voltage-gated Ca^{2+} currents were evoked by delivering voltage steps at different times during run-down of the response. The largest response was obtained by evoking three currents in rapid succession. In this Fig. (and Fig. 4*A*) the fluorescence in the soma was measured over successive 500 ms intervals and each point was normalized with respect to the 3–4 images obtained immediately prior to the voltage step. The timing of the voltage steps is denoted by the bar. (Note that in *Aa* (and Fig. 8*A*) at the early time points Cs^+ had not fully blocked the K^+ currents; this would incur a small error (~ 5%) in the calculation of charge associated with Ca^{2+} entry.)

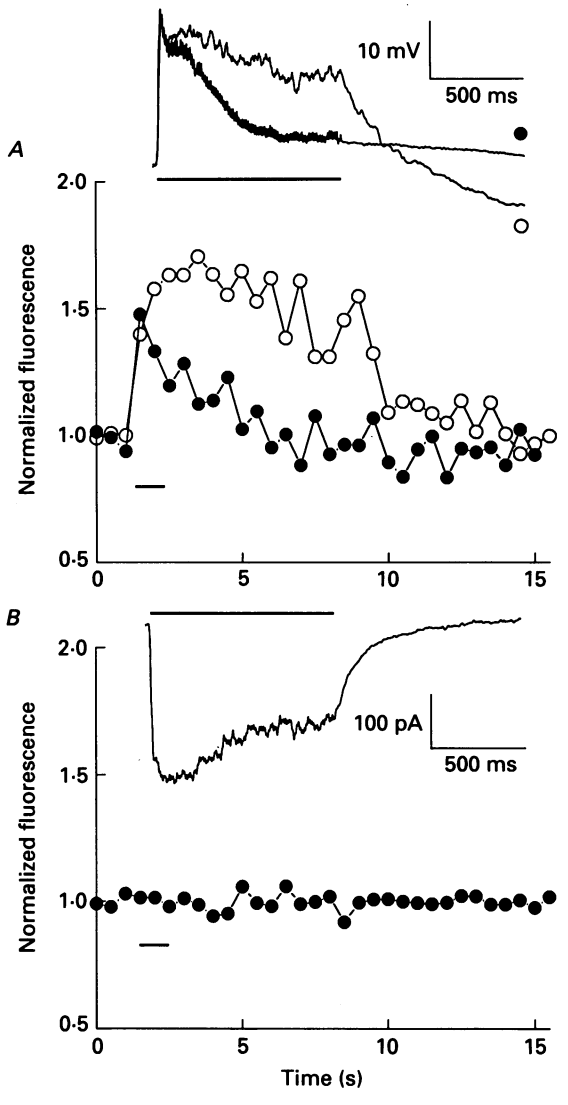

Fig. 3. Somatic Ca^{2+} transients in response to synaptic activation. *A*, the graph plots the somatic Ca^{2+} transient evoked by a tetanus under control conditions (○) and in the presence of 100 μM AP5 (●). The traces above are the corresponding synaptic potentials. Note that AP5 dramatically reduces the latter part of the synaptic potential and shortens the duration of the Ca^{2+} transient. The membrane potential of the cell was set to −70 mV prior to the tetanus. *B*, the graph shows no change in fluorescence, measured at the soma of the same cell prior to the addition of AP5, when the tetanus was delivered while the neurone was voltage clamped, at −70 mV. The trace shows the corresponding synaptic current. In these experiments the patch-pipette contained K^+, rather than Cs^+, to enable repolarization following the tetanus. The after-hyperpolarization following the tetanus is not seen if Cs^+ is used and is presumably the result of Ca^{2+}-activated K^+ channel activity. In this and subsequent figures, the duration of the tetanus is denoted by a bar. In some of the electrophysiological records there is a thickening of the trace during the tetanus due to incompletely removed stimulus artifacts. The plots of fluorescence are normalized with respect to the 3–4 images obtained immediately prior to the tetanus.

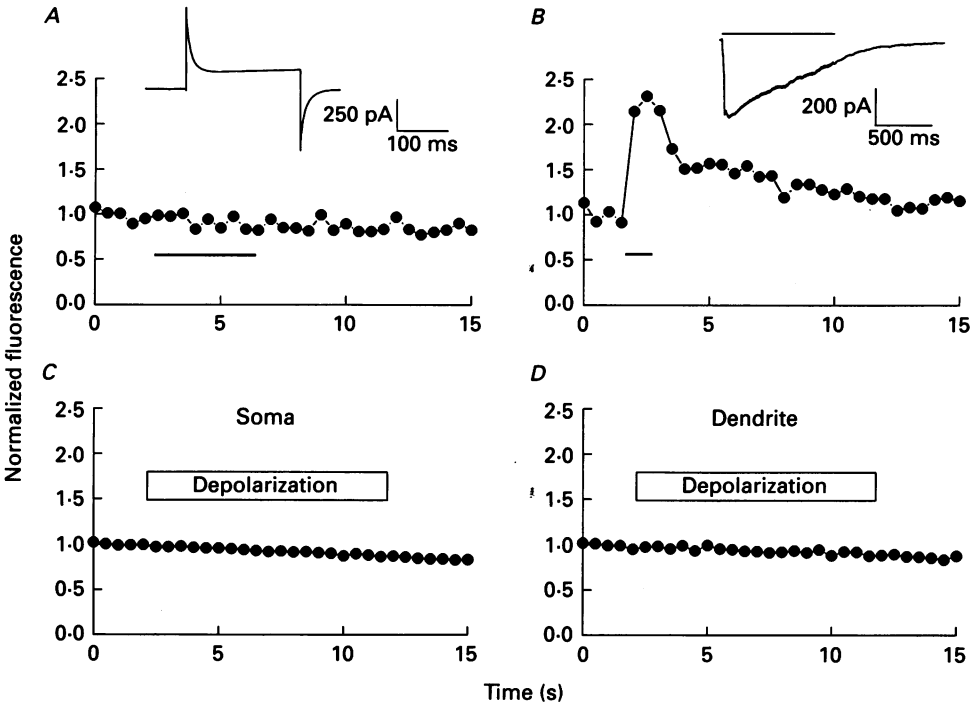

Fig. 4. Dendritic Ca^{2+} transients are elicited by synaptic activation but not by voltage steps. *A*, the graph shows no change in fluorescence in response to 10 successive 200 ms voltage steps from −70 to 0 mV, delivered at 500 ms intervals. The trace illustrates a typical current response to one of these voltage steps. *B*, tetanic stimulation induced a Ca^{2+} transient in the same dendritic region of the cell from which the measurements in *A* were obtained. The trace shows the corresponding synaptic current. The cell was voltage clamped at −35 mV. *C* and *D* show the absence of fluorescence changes in either the soma (*C*) or dendrites (*D*) when the Cs^{+}-filled neurone was rapidly depolarized by switching from voltage-clamp (at −60 mV) to current-clamp ($I = 0$), for the duration of the box above the graph. In both cases the neurone depolarized rapidly to −10 mV.

Fig. 5. *A*. An optical section (obtained at the end of the experiment) of a neurone. The superimposed box (width 40 μm) denotes the region from where fluorescence measurements were made during the experiment. The scale bar denotes 50 μm. *B*, images of this dendritic segment, each obtained over a 500 ms period, during the course of the experiment; prior to the tetanus, at the peak of fluorescence and at two time points during the decay phase of the response. The circular 'hot spots' visible in *A*, but not in *B*, may be a consequence of neuropathological change since maximally fluorescent images of the patch-clamped neurones were obtained at the end of the experiment by withdrawing the patch pipette. Presumably this allowed a massive influx of Ca^{2+} into the cell via the site of whole-cell access. Such localized regions of sustained elevations in dendritic Ca^{2+} were never observed during data collection periods. *C*, dendritic Ca^{2+} transient and associated synaptic current from this cell, voltage-clamped at −35 mV. The numbers 1–4 correspond to the images illustrated in *B*. *D*, pooled data from all twenty-eight neurones from which dendritic images were obtained in response to a tetanus delivered at a holding potential of −35 mV.

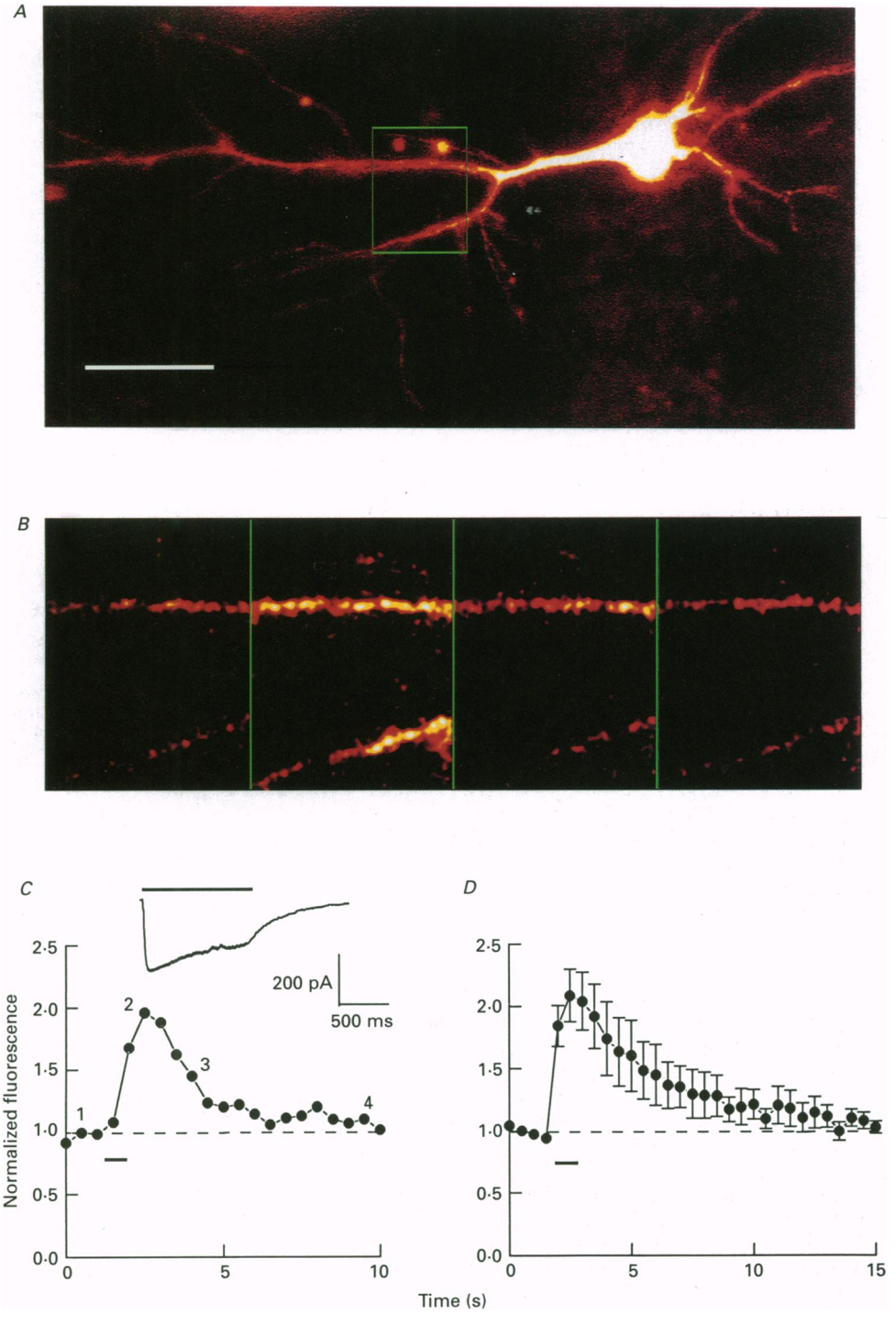

Fig. 5. For legend see facing page.

Ca^{2+} transients in the dendrites

By the time that sufficient dye had diffused into the dendrites to enable images of sufficient intensity for accurate dendritic fluorescence measurements to be obtained, voltage steps did not produce Ca^{2+} currents or fluorescence transients in any part of

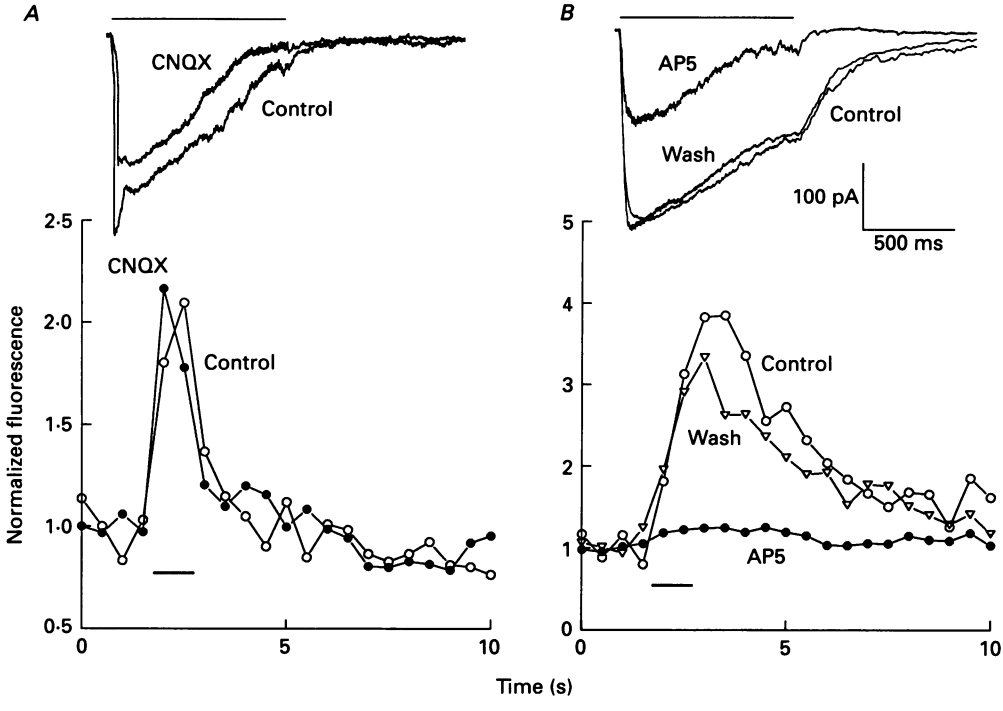

Fig. 6. The effects of excitatory amino acid receptor antagonists on dendritic Ca^{2+} transients. *A*, CNQX has no effect on tetanus-induced dendritic Ca^{2+} transients. The graph plots responses, obtained at a holding potential of −35 mV, in the presence (●) and absence (○) of 10 μM CNQX. The respective synaptic currents are superimposed and show that CNQX slows the initial rise and reduces the current throughout the tetanus. *B*, AP5 greatly reduces tetanus-induced dendritic Ca^{2+} transients. The graph plots responses from a different neurone, obtained at a holding potential of −35 mV, before (○), during (●) and following wash-out (▽) of 100 μM AP5. The respective synaptic currents are superimposed and show that AP5 does not affect the initial rise but reduces the current throughout and following the tetanus.

the cell (Fig. 4*A*). Furthermore, rapidly depolarizing the Cs^+-loaded cell by switching from voltage-clamp (at −60 mV) to current-clamp ($I = 0$) also failed to elicit fluorescence transients in either the soma or dendrites (Fig. 4*C* and *D*). (Note that when K^+ conductances are blocked following Cs^+ loading the resting membrane potential is close to 0 mV). In contrast, tetanic stimulation (100 Hz, 1 s) resulted in a transient increase in cytosolic free Ca^{2+} in the dendrites of all neurones examined, recorded under either current-clamp ($n = 3$) or voltage-clamp ($n = 30$) conditions (Fig. 4*B*, Fig. 5). In twenty eight cells voltage clamped at −35 mV the fluorescence,

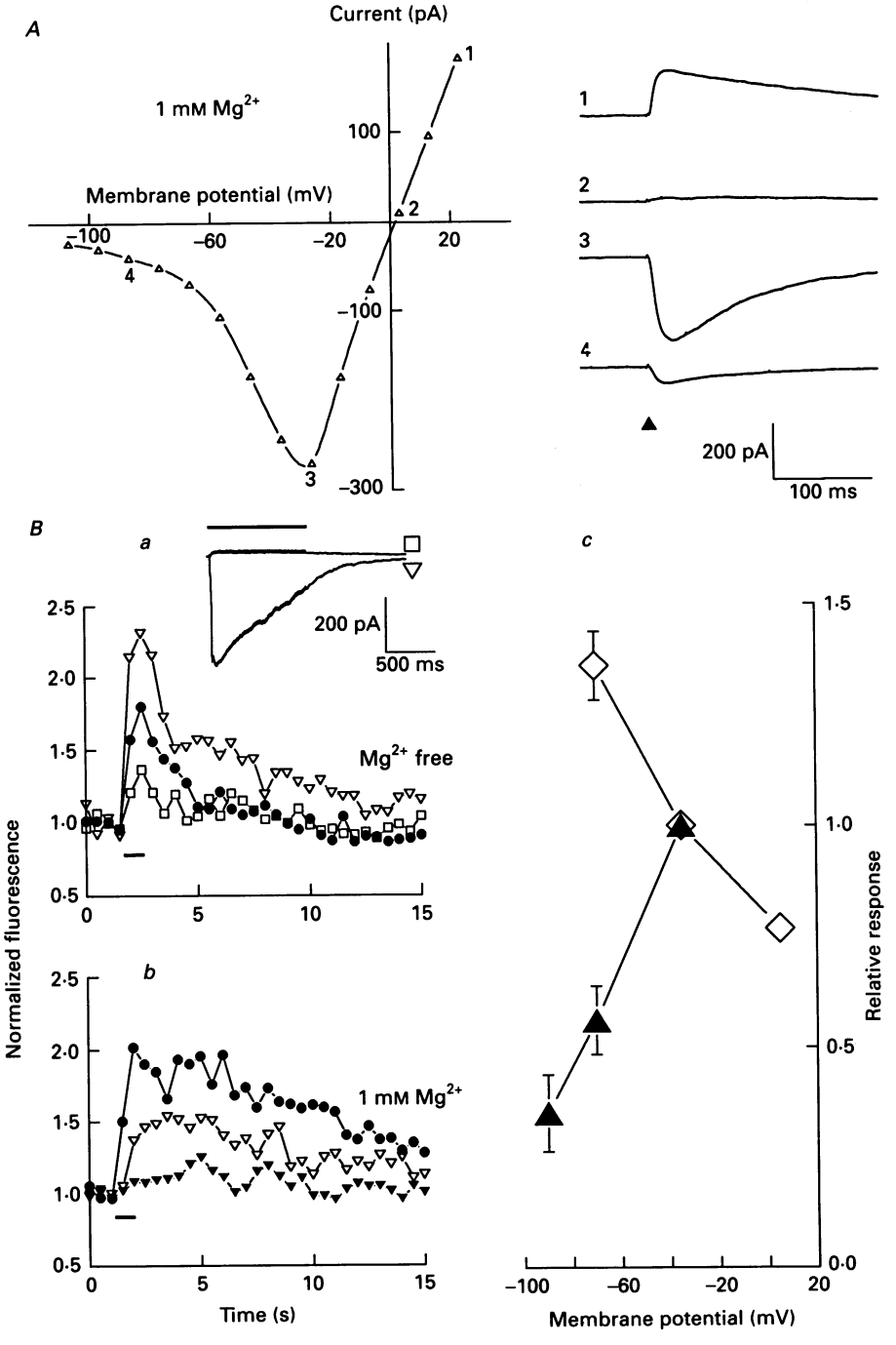

Fig. 7. The voltage dependence of NMDA receptor-mediated synaptic currents and dendritic Ca^{2+} transients. *A*, NMDA receptor-mediated EPSCs were evoked by low-frequency stimulation of the Schaffer collateral–commissural pathway in the presence of 10 μM CNQX, to block the AMPA receptor-mediated synaptic component. The graph plots the peak synaptic current *versus* the holding potential. Averages of four consecutive synaptic currents are illustrated at the membrane potentials indicated on the graph by

measured in 53 μm lengths of apical dendrite, increased to $209 \pm 21\%$ of control during (or shortly after) the tetanus and then decayed back to baseline values over a period of several seconds ($t_{\frac{1}{2}}$ of $5{\cdot}1 \pm 0{\cdot}9$ s). Pooled data from these twenty-eight cells are illustrated in Fig. 5*D*.

To investigate which receptors mediate the tetanus-induced synaptic Ca^{2+} transients, experiments were performed in the presence of the selective AMPA receptor antagonist CNQX or the specific NMDA receptor antagonist AP5 (Fig. 6). 10 μM CNQX, which under the conditions of the present experiments selectively blocks responses mediated through the activation of AMPA receptors (Blake, Yates, Brown & Collingridge, 1989), did not affect the Ca^{2+} transients ($n = 3$; Fig. 6*A*). In contrast, 100 μM AP5 greatly reduced or abolished the Ca^{2+} transients in a reversible manner (Fig. 6*B*). The mean reduction in the increase in fluorescence (measured at the end of the tetanus) was $82 \pm 6\%$ ($n = 3$). Both compounds reduced the tetanus-induced synaptic current (Fig. 6), as would be expected since both receptor types contribute to the synaptic excitation of these neurones (Davies & Collingridge, 1989).

Before investigating the voltage dependence of the dendritic Ca^{2+} transients, we assessed the ability of the patch pipette to provide DC clamp of the synaptic region. The *I–V* profile of pharmacologically-isolated NMDA receptor-mediated synaptic currents (Fig. 7*A*) demonstrate good DC clamp of the dendrites where the synaptic conductances originate. In 1 mM Mg^{2+}-containing medium, over the membrane potential range of -35 to -90 mV, the dendritic Ca^{2+} transients were greater when tetani were delivered at more depolarized potentials (Fig. 7*B*). In contrast, in slices perfused for at least 1 h with medium to which Mg^{2+} had been omitted, the voltage dependence was conventional (Fig. 7*B*). Two of these slices were held at a positive membrane potential such that the tetanus induced a small outward current; in both cases there was a small Ca^{2+} transient (Fig. 7*B*). The voltage dependence conferred by Mg^{2+} and the separation of the reversal potentials of the Ca^{2+} component from the total current are in complete accord with a signal initiated by Ca^{2+} permeation through NMDA channels (Mayer *et al.* 1987; Ascher & Nowak, 1988).

Collectively, the pharmacology and voltage dependence of the dendritic Ca^{2+} transient and the failure of voltage steps to elicit dendritic Ca^{2+} transients suggests strongly that Ca^{2+} entry through voltage-gated Ca^{2+} channels does not make any significant contribution to the dendritic signals recorded. As a further test, tetanic stimulation was delivered to three cells in the presence of 10 μM nitrendipine, a treatment which blocked reversibly voltage-gated Ca^{2+} currents evoked by voltage steps from -35 mV (Fig. 8*A*). The dendritic transients evoked at a holding potential

---

the numbers (1–4). *B*, Mg^{2+}-conferred voltage dependence of dendritic Ca^{2+} transients. *Ba*, conventional voltage dependence in Mg^{2+}-free medium. Dendritic Ca^{2+} transients were induced by tetanic stimulation delivered at three holding potentials after perfusion for at least 60 min with medium containing no added Mg^{2+} (□, +5 mV; ●, −35 mV; ▽, −70 mV). The traces are the corresponding synaptic currents at +5 and −70 mV. *Bb*, anomalous voltage dependence in the presence of 1 mM Mg^{2+}. Dendritic Ca^{2+} transients were induced in a different neurone by tetanic stimulation delivered at three holding potentials (●, −35 mV; ▽, −70 mV; ▼, −90 mV). *Bc*, the graph plots pooled data for neurones recorded in the presence (▲) or absence (◇) of added Mg^{2+}. The Ca^{2+} signal was expressed relative to that evoked at −35 mV. Each point plots the means ± S.E.M. values for between two and six neurones.

of −35 mV, were indistinguishable from those obtained under control conditions. Thus, in the presence of nitrendipine, tetanic stimulation caused an increase in dendritic Ca^{2+} fluorescence to 250±82% of control (Fig. 8*C*). As in control medium, the dendritic Ca^{2+} transients were smaller at −70 mV than at −35 mV (Fig. 8*B*), the value at −70 mV being 39±5% of that at −35 mV ($n = 3$).

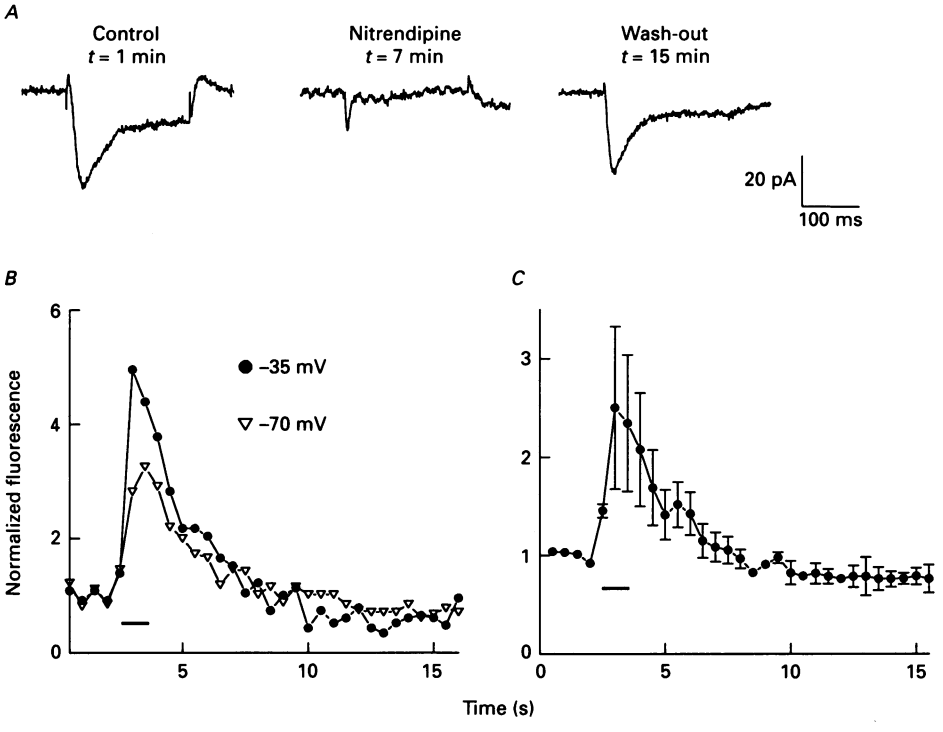

Fig. 8. The effect of nitrendipine on Ca^{2+} signalling. *A*, the traces show the currents evoked by a voltage step from −35 to 0 mV at the times indicated following the obtainment of whole-cell access. Nitrendipine (10 μM) applied for 5 min at $t = 2$ min abolished, in a reversible manner, the slow inward current. *B* and *C*, tetanic stimulation-induced dendritic Ca^{2+} transients in the presence of 10 μM nitrendipine. *B* plots the response of one cell to tetani delivered at two different membrane potentials. *C* plots pooled data from three cells obtained at a membrane potential of −35 mV.

Ca^{2+}-induced Ca^{2+} release contributes to the dendritic Ca^{2+} transient

The decay time of the tetanus-induced Ca^{2+} transient was variable between cells (compare *A* and *B* of Fig. 6). One possibility for this variability is a secondary process which prolongs the initial Ca^{2+} signal. To assess this possibility further, small (*circa* 4 μm) adjacent sections of dendrite were analysed in more detail. In cells showing prolonged decay times, the analysis of these small segments revealed oscillatory behaviour (Fig. 9). Neighbouring segments oscillated to different degrees and there was no obvious synchrony between segments. The oscillations were smaller in the absence of tetanic stimulation (not illustrated) or following tetanic stimulation in the presence of 100 μM AP5 (Fig. 9*C*).

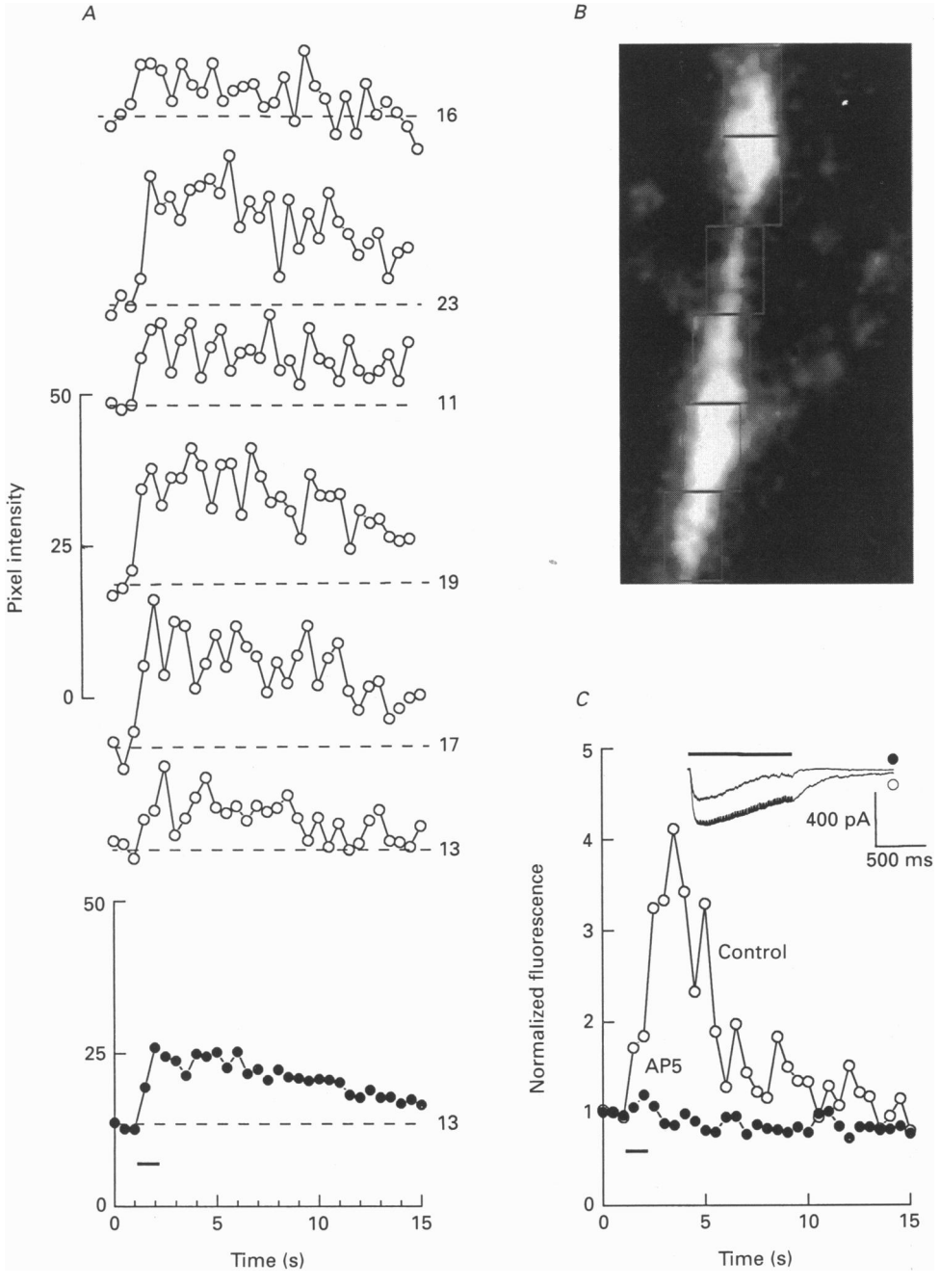

Fig. 9. Tetanus-induced elevations of dendritic Ca^{2+} display localized oscillatory behaviour. *A*, the upper six graphs (○) plot the Ca^{2+} transients in the corresponding six boxes shown in *B* and the lower graph (●) is the Ca^{2+} transient measured over the whole length of the dendrite. The boxes are 4 μm in width. The absolute fluorescence is plotted (in arbitrary units) and the numbers indicate the resting fluorescence intensity (to enable the signal to be related to the absolute fluorescence). Note the marked oscillations in the

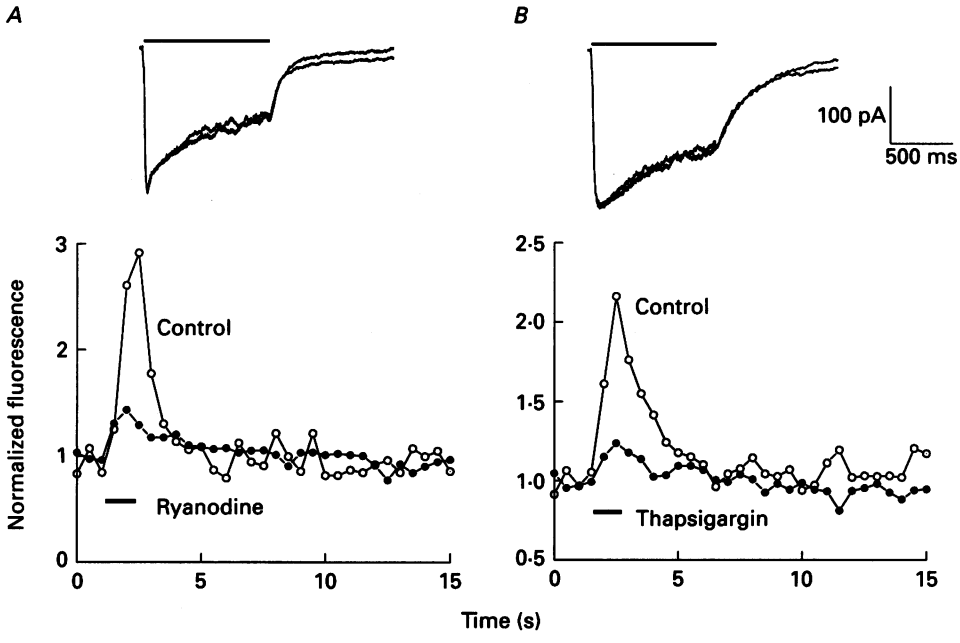

Fig. 10. The dendritic Ca^{2+} transient is largely due to Ca^{2+} release from intracellular stores. *A*, ryanodine greatly depressed the Ca^{2+} transient without affecting the synaptic current induced by a tetanus delivered while the cell was held at −35 mV. The graph plots the control response (○) and the response to the second tetanus delivered in the presence of 10 μM ryanodine (●). The corresponding synaptic currents are superimposed to show the lack of effect of ryanodine. *B*, thapsigargin greatly depressed the Ca^{2+} transient without affecting the synaptic current induced by a tetanus in a different cell held at −35 mV. The graph plots the control response (○) and the response to the second tetanus delivered in the presence of 10 μM thapsigargin (●). The corresponding synaptic currents are superimposed to show the lack of effect of thapsigargin.

One explanation for the oscillations is that the signal involves a component due to Ca^{2+}-induced Ca^{2+} release (Tsien & Tsien, 1990). Experiments were performed, therefore, using ryanodine which blocks this process (Thayer, Hirning & Miller, 1988) and thapsigargin, which depletes most intracellular Ca^{2+} pools via inhibition of the Ca^{2+}-ATPase (Thastrup, Cullen, Drobak, Hanley & Dannies, 1990). In each cell, treatment with either 10 μM ryanodine or 10 μM thapsigargin depressed the peak of the Ca^{2+} transients (to 33 ± 7 ($n = 4$) and 36 ± 7 ($n = 2$) % of control, respectively) without affecting the tetanus-induced synaptic currents (Fig. 10). Thapsigargin also

small dendritic sections, which are much less evident when the measurement is made over a large area. *C*, oscillations in dendritic Ca^{2+} recorded from a 4 μm segment of dendrite of a cell, voltage clamped at −35 mV, in response to tetani delivered under control conditions (○) and in the presence of 100 μM AP5 (●). Note that AP5 both substantially reduces the Ca^{2+} rise during the tetanus and the oscillations in the Ca^{2+} signal following the tetanus. The inset shows the corresponding tetanus-induced synaptic currents.

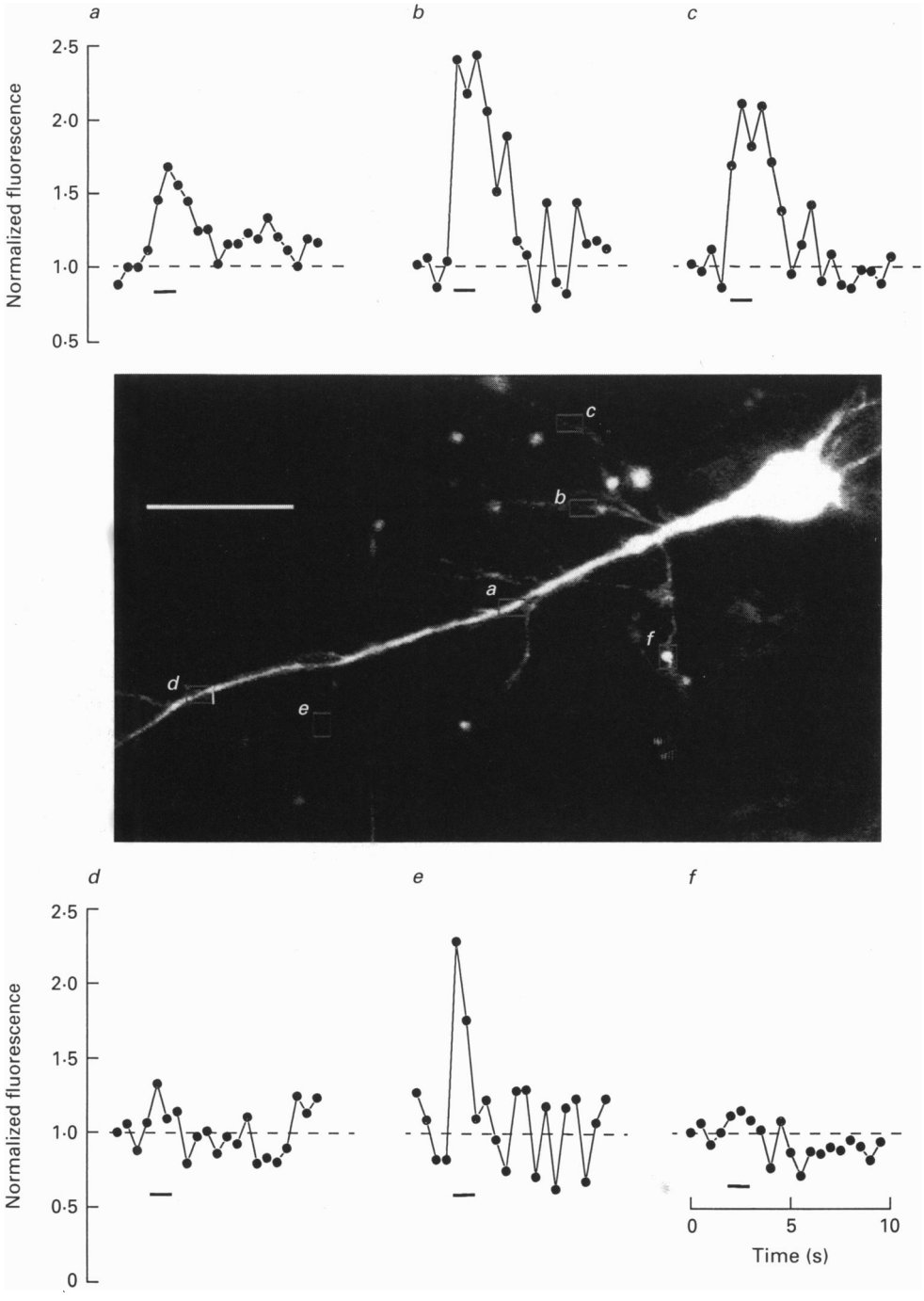

Fig. 11. Heterogeneity in Ca^{2+} signals in the dendritic tree of a neurone. Each graph (*a–f*) plots the Ca^{2+} transient for the corresponding dendritic region, as indicated on the image, in response to a tetanus delivered whilst the neurone was voltage clamped at −35 mV. Note the larger changes in the Ca^{2+} signal in the finer processes, compared with the main dendritic trunk. The absence of a Ca^{2+} response at *d* and *f* may reflect the lack of an active synaptic connection in this region. The image was obtained at the end of the experiment after withdrawal of the patch pipette. Scale bar measures 50 μm.

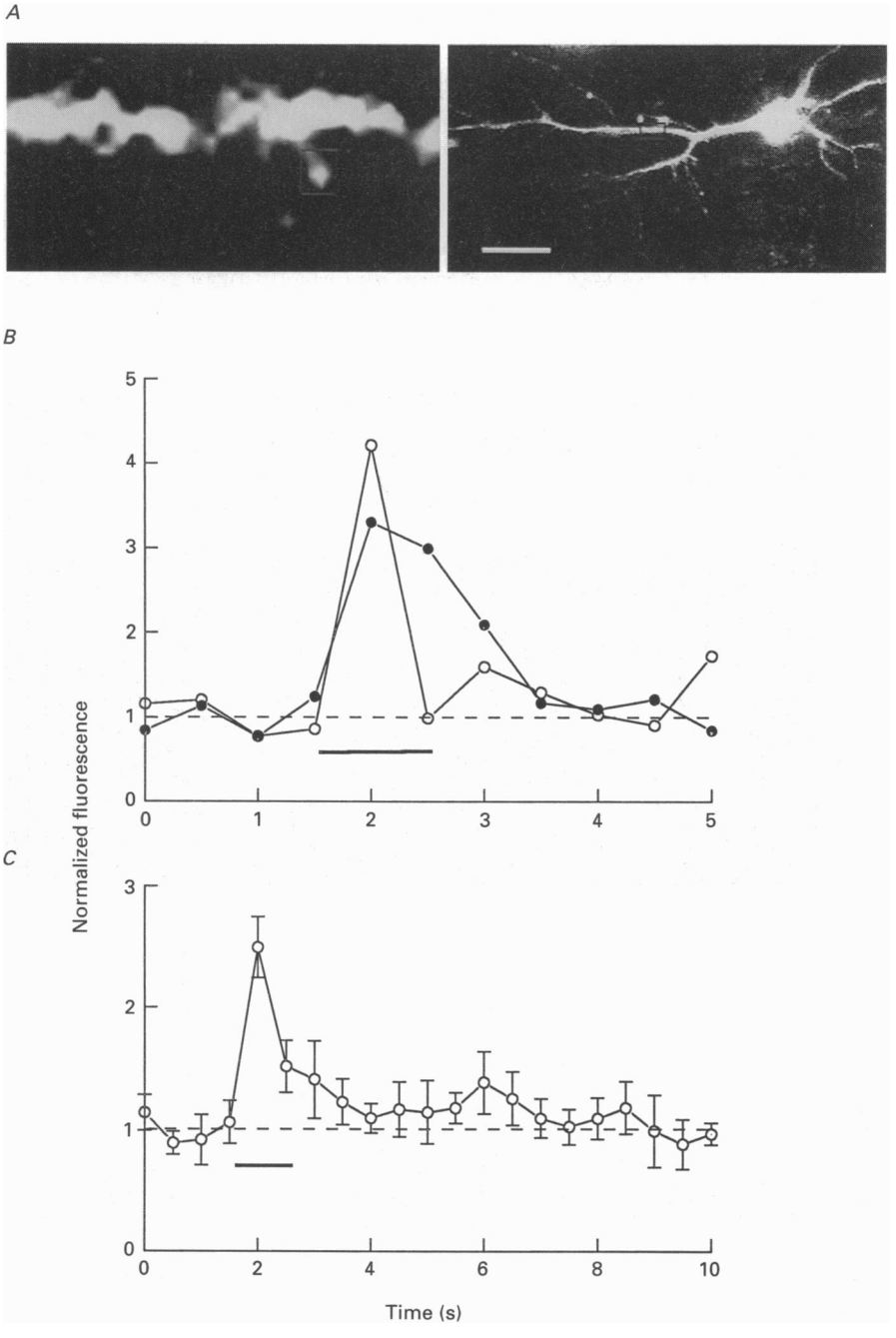

Fig. 12. Tetanus-induced Ca^{2+} transients in spine-like processes. The left-hand image shows an enlarged view of a section of the main dendrite with a clearly visible spine-like protuberance (enclosed by the box, box width 1 μm). The right-hand image shows the neurone and indicates the location of this region of dendrite (enclosed by the box). The scale bar denotes 50 μm. *B* plots the tetanus-induced Ca^{2+} transient in the 'spine' illustrated in *A* (○) and also the Ca^{2+} transient in the adjacent region of dendrite (●) under control conditions. *C* shows pooled data for the tetanus-induced Ca^{2+} rise in six 'spines' measured from two neurones recorded in the presence of CNQX.

reduced the peak of the Ca^{2+} transients (to 71 and 88% of control, $n = 2$) when applied at 100 nM (not illustrated).

The localization of the dendritic Ca^{2+} transients

The tetanus-induced rise in dendritic Ca^{2+} was restricted to a band of approximately 100 μm and corresponded to the region of the dendrites adjacent to the stimulating electrode. Within these bands there was considerable heterogeneity (Fig. 11), suggesting that the Ca^{2+} signal was compartmentalized to those regions receiving synaptic inputs. In a few neurones the resolution was sufficient to detect spine-like processes on the dendrites. Within these 'spines' the Ca^{2+} signals decayed back to baseline within a few seconds of the tetanus (Fig. 12). Sustained Ca^{2+} transients in the 'spines' were not observed.

DISCUSSION

The present results have revealed several distinct Ca^{2+} signalling mechanisms that are evoked by the synaptic activation of NMDA receptors. Before discussing these signalling pathways a consideration of the techniques is presented since electrophysiological and Ca^{2+}-imaging techniques have not previously been combined in this manner for the recording of neuronal activity within slices of brain tissue.

The use of confocal microscopy for measuring changes in Ca^{2+} concentration

The primary reason for using a confocal microscope was to prevent light from out-of-focus regions of the neurone from contaminating the image within the focal plane. This reduces glare thereby improving both image quality and resolution. We consider that the changes in fluorescence that we have measured are due to alterations in Ca^{2+} concentration *per se*, rather than alterations in dye concentration or path length, for several reasons. Firstly, there were no detectable changes in cell morphology; secondly, dendritic measurements were integrated over a volume sufficient to compensate for the possibility of subtle changes in morphology or dye compartmentalization; and thirdly, depolarizing steps led to increases in fluorescence in proportion to the size of the Ca^{2+} currents evoked. Since the distribution of dye within an optical section and the light path vary, estimates of spatial variation of Ca^{2+} within one optical section are not meaningful. However, on the reasonable assumption that these parameters are invariant for each point during the 10–20 s of an experimental data collection period then temporal information of Ca^{2+} changes at given locations can be obtained. In this way comparisons between temporal profiles of different areas can be made. However, it is not possible to calculate the absolute physiological Ca^{2+} concentrations because these values will be influenced by the dialysis of the neurone with the patch solution, a limitation which applies similarly to ratiometric imaging. For this reason we have expressed the data relative to the pre-stimulus intensities. An advantage of fluo-3 over ratiometric dyes such as fura-2 is its more appropriate dissociation constant for measuring physiological Ca^{2+} transients and its higher quantum yield. As a consequence the Ca^{2+} signal will be less distorted by the dye. Ca^{2+} transients evoked by control tetani did not alter

appreciably in profile as the dye concentration in the dendrites increased. This suggests that any perturbation of the signal by fluo-3 was minimal under the conditions of the present experiments.

The use of patch-clamp techniques

Whole-cell patch-clamp techniques were used for three complementary purposes. The first was to monitor the electrophysiological viability of the neurone and to correlate, in real time, the Ca^{2+} signals with concomitant synaptically evoked and intrinsic responses.

The second purpose was to dialyse extensively the neurones with a solution which did not provide ATP support and thereby remove the complications which may otherwise arise from voltage-gated Ca^{2+} channels. It should be stressed, however, that although the absence of ATP support completely compromised Ca^{2+} channel activity, other ATP-dependent functions, such as the filling of intracellular Ca^{2+} stores, were not affected. This presumably reflects different requirements for ATP and/or compartmentalization of the ATP-dependent processes, together with the ability of the neurones to generate some ATP. Other ATP-dependent processes, such as GABA-mediated synaptic inhibition, together with most voltage-dependent conductances were deliberately eliminated pharmacologically to simplify interpretation of results. The AMPA and NMDA receptor-mediated synaptic responses did not exhibit run-down during the period that measurements were made.

The third purpose of whole-cell recording was to control the membrane potential. In this respect, we assessed the fidelity of the clamp in several ways. The DC clamp was tested by determining the voltage dependence of pharmacologically isolated NMDA receptor-mediated synaptic currents, in the presence of 1 mM Mg^{2+}, between -100 and $+30$ mV. As has been reported previously (Hestrin, Nicoll, Perkel & Sah, 1990; Konnerth, Keller, Ballanyi & Yaari, 1990; Randall, Schofield & Collingridge, 1990) the voltage dependence was very similar to that of NMDA channels recorded in detached patches (Ascher & Nowak, 1988). Therefore, it can be concluded that the DC clamp is adequate to provide, for example, steady-state inactivation of any residual low-threshold voltage-gated Ca^{2+} channels. The settling of the clamp was determined by evoking synaptic currents during voltage steps, of the sort used to elicit Ca^{2+} currents. The clamp attained the desired potential within 10 ms of the start of the step (the earliest time point tested; data not shown).

Ca^{2+} entry through voltage-gated Ca^{2+} channels

In the present experiments, the entire tetanus-induced Ca^{2+} rise in the soma was due to entry via voltage-gated channels. Under the conditions of the present experiments this component could only be recorded soon after obtaining whole-cell access, due to the rapid run-down of the voltage-gated Ca^{2+} conductances. The failure to detect Ca^{2+} permeation through NMDA channels in the soma is consistent with the lack of direct excitatory innervation of the soma, despite a high density of somatic NMDA channels (Randall, Benke, Angelides, Schofield & Collingridge, 1990; Gibb & Colquhoun, 1991). It shows further that Ca^{2+} permeating NMDA channels on the dendrites is unable to reach the soma. The present work does not preclude a role for dendritic voltage-gated Ca^{2+} channels in Ca^{2+} signalling (Regehr & Tank, 1992).

Additional experiments, where these have not been deliberately eliminated, will be required to address this issue.

Ca^{2+} permeation through NMDA channels

The use of whole-cell recording has enabled the component of the Ca^{2+} signal due to permeation through NMDA channels to be recorded without contamination by Ca^{2+} entry through voltage-gated channels. We obtained confirmation that voltage-gated Ca^{2+} channel activity did not contaminate the dendritic Ca^{2+} transients in several ways. In all experiments, the synaptic current evoked by the tetanus was recorded. Initially when sufficient dye had reached the dendrites to enable their visualization there were often still signs of voltage-gated Ca^{2+} channel activity evoked by tetanic stimulation. This activity disappeared with time and measurements were not obtained until any sign of contamination by voltage-gated currents had disappeared. At this time, nitrendipine, which abolished all voltage-gated Ca^{2+} channel activity evoked by voltage steps from -35 mV, had no effect on tetanus-induced Ca^{2+} transients. In addition, AP5, but not CNQX, reduced, substantially, the synaptically evoked Ca^{2+} transients; had voltage breakthrough posed a problem then the faster CNQX-sensitive, AP5-resistant EPSPs should have been the major contributor. The dependence of the Ca^{2+} transients on voltage and Mg^{2+}, is difficult to explain on the basis of entry through voltage-gated Ca^{2+} channels but is entirely consistent with entry through NMDA channels (Mayer *et al.* 1987; Ascher & Nowak, 1988). In particular the Ca^{2+} transient recorded at a positive potential, where voltage-gated Ca^{2+} channels are inactivated and any synaptic voltage breakthrough would be in the hyperpolarizing direction, cannot possibly involve voltage-gated Ca^{2+} channels.

Since the dendritic Ca^{2+} transients were substantially inhibited by AP5 but were unaffected by CNQX, it can be concluded that Ca^{2+} permeation through AMPA channels (Iino, Ozawa & Tsuzuki, 1990; Hollmann, Hartley & Heinemann, 1991) did not contribute to the signals recorded in the present experiments. The small residual Ca^{2+} signal sometimes seen in the presence of AP5 can probably be accounted for by its competitive nature and the large amounts of L-glutamate released by tetanic stimulation.

Magnification of the signal by Ca^{2+}-induced Ca^{2+} release

A surprising observation was the extent to which the Ca^{2+} signal that permeates NMDA channels is magnified by a ryanodine- and thapsigargin-sensitive process. Previous studies have suggested that the Ca^{2+} signal induced by the application of NMDA to cultured neurones contains a major component due to Ca^{2+}-induced Ca^{2+} release (Mody, MacDonald & Baimbridge, 1988; Segal & Manor, 1992). However, this is the first demonstration, to our knowledge, that the Ca^{2+} signal initiated by Ca^{2+} permeation directly through NMDA channels involves magnification by Ca^{2+} release from intracellular stores. Furthermore, this study demonstrates the mobilization of intracellular Ca^{2+} stores following the transient synaptic activation of NMDA receptors. In the present study we have used high concentrations of ryanodine and thapsigargin (10 μM) with the intention of eliminating the component of the signal due to Ca^{2+} release from intracellular stores (Irving, Collingridge & Schofield, 1992).

Therefore, it can be concluded that Ca^{2+}-induced Ca^{2+} release accounts for approximately 65% of the total signal, recorded under the present conditions. At 100 nM, thapsigargin produced a smaller reduction in the Ca^{2+} transient; this dose dependency correlates with the ability of thapsigargin to inhibit Ca^{2+} mobilization in neurones (Irving *et al.* 1992). This Ca^{2+}-induced Ca^{2+} release mechanism provides a second level of non-linearity to the NMDA receptor system, in addition to the voltage dependence of the NMDA receptor system conferred by Mg^{2+}.

It is possible that the oscillations observed in small segments of dendrites reflect this Ca^{2+}-induced Ca^{2+} release mechanism. Consistent with this possibility was the finding that they were largely dependent upon the synaptic activation of NMDA receptors. The fast frequency of the oscillations, that could not be fully resolved in the present study, may reflect the small distances within the fine dendritic processes that Ca^{2+} has to diffuse across to release additional Ca^{2+}. The variability between cells of the extent of these oscillations may reflect small differences in the level of Ca^{2+} buffering.

Ca^{2+} signalling and LTP

The use of electrophysiological techniques has enabled us to ensure that all measurements were made on viable neurones and to exclude, therefore, the possibility that the Ca^{2+} signals are correlates of pathological changes. However, the extensive dialysis and sustained activation of the NMDA receptor system eliminated the ability of the cells to exhibit LTP. This has the advantage that it enabled all measurements to be made on neurones at a fixed synaptic strength. Although a direct correlation between Ca^{2+} measurements and LTP was not possible, a comment on the observed Ca^{2+} signalling and LTP is in order.

The Ca^{2+} entry through voltage-gated Ca^{2+} channels on the soma, though activated by dendritic NMDA receptor-mediated EPSPs, is unlikely to play a major role in the early stages of LTP since entry of Ca^{2+} through voltage-gated Ca^{2+} channels *per se* does not induce persistent LTP (Kullmann, Perkel, Manabe & Nicoll, 1992) and LTP lasting approximately 3 h can be induced in a slice preparation from which the CA1 cell bodies have been removed (Frey, Krug, Brodemann, Reymann & Matthies, 1989). The possibility remains, however, that this somatic Ca^{2+} signal could be involved in later stages of LTP, perhaps initiating a message to the nucleus to alter protein synthesis (Hernandez-Cruz, Sala & Adams, 1990).

The Ca^{2+} that permeates NMDA channels is believed to provide the initial trigger for LTP. The high degree of localization of the Ca^{2+} signal is consistent with the popular notion that restricted diffusion of Ca^{2+} following its entry through NMDA channels provides the basis for the property of synapse specificity. In the present study, this signal, even within very small spine-like structures, was transient and contrasts, therefore, with the recent report that Ca^{2+} stays elevated for long periods following tetanic stimulation (Müller & Connor, 1991). There are several possible explanations for this discrepancy. Firstly, the presence of dendritic voltage-gated Ca^{2+} channels may elevate dendritic Ca^{2+} to such an extent that the Ca^{2+} extrusion, sequestration and buffering mechanisms are overwhelmed. Secondly, sustained Ca^{2+} elevations may reflect pathological, rather than physiological, changes. Since, in the study of Müller & Connor (1991), electrophysiological measurements were not made

simultaneously with the imaging of Ca^{2+}, these and other possibilities cannot be distinguished. With respect to the induction of LTP, experiments using the photolabile Ca^{2+} buffer diazo-4 suggest that the Ca^{2+} rise need only last a few seconds (Malenka, Lancaster & Zucker, 1992).

It is likely that the amplification of the Ca^{2+} signal which permeates NMDA channels by Ca^{2+} release from intracellular stores is involved in the generation of LTP, since thapsigargin interferes with the induction of LTP (Harvey & Collingridge, 1992; Bortolotto & Collingridge, 1993) over the same concentration range that it reduces the NMDA receptor-mediated Ca^{2+} transient. The extent to which this magnification directly involves Ca^{2+}-induced Ca^{2+} release as opposed to inositol 1,4,5-trisphosphate-induced release is unclear since attempts to address this issue using dantrolene have led to equivocal results (Obenaus, Mody & Baimbridge, 1989; Xu & Krnjevic, 1990).

Concluding remarks

In summary, our results have shown that high-frequency synaptic activation of the NMDA receptor can elevate Ca^{2+} in neurones by a variety of routes and they demonstrate the need to combine imaging and voltage-clamp plus intracellular dialysis techniques to separate these pathways. Using this approach we have been able to visualize, in real time, the Ca^{2+} signal which is believed to provide the essential trigger for the induction of LTP.

We are extremely grateful to Professors J. B. Chappell and O. T. G. Jones for the use of their BioRad MRC 500 confocal microscope for the initial experiments performed between 1990 and 1991; this was provided by a grant from the Wellcome Trust. We are also most grateful to the University of Birmingham for purchasing the BioRad MRC 600 which was used in the subsequent experiments. We thank Professor J. C. Watkins for the gifts of AP5 and CNQX and Andy Randall for advice and assistance. We are most grateful to the Wellcome Trust for financial support throughout.

REFERENCES

ALFORD, S. & COLLINGRIDGE, G. L. (1990*a*). Somatic Ca^{2+} entry following repetitive synaptic stimulus in patch-clamped CA1 pyramidal neurons in rat hippocampal slices. *Journal of Physiology* **435**, 44*P*.

ALFORD, S. & COLLINGRIDGE, G. L. (1990*b*). Simultaneous whole-cell patch-clamp recording and imaging of single pyramidal neurons in rat hippocampal slices. *Journal of Physiology* **435**, 5*P*.

ALFORD, S., FRENGUELLI, B. G. & COLLINGRIDGE, G. L. (1992). Ca^{2+} release from intracellular stores magnifies the Ca^{2+} signal which permeates dendritic NMDA channels following synaptic activation of CA1 hippocampal neurones *in vitro*. *Journal of Physiology* **452**, 178*P*.

ALFORD, S., SCHOFIELD, J. G. & COLLINGRIDGE, G. L. (1991). Dendritic Ca^{2+} transients associated with NMDA receptor-mediated synaptic currents in rat hippocampal slices. *Journal of Physiology* **438**, 255*P*.

ASCHER, P. & NOWAK, L. (1988). The role of divalent cations in the *N*-methyl-D-aspartate responses of mouse central neurones in culture. *Journal of Physiology* **399**, 247–266.

BLAKE, J. F., YATES, R. G., BROWN, M. W. & COLLINGRIDGE, G. L. (1989). 6-Cyano-7-nitroquinoxaline-2,3-dione as an excitatory amino acid antagonist in area CA1 of rat hippocampus. *British Journal of Pharmacology* **97**, 71–76.

BLANTON, M. G., LOTURCO, J. J. & KREIGSTEIN, A. R. (1989). Whole-cell recording from neurons in slices of reptilian and mammalian cerebral cortex. *Journal of Neuroscience Methods* **30**, 203–210.

BLISS, T. V. P. & COLLINGRIDGE, G. L. (1993). A synaptic model of memory: long-term potentiation in the hippocampus. *Nature* **361**, 31–39.

BORTOLOTTO, Z. A. & COLLINGRIDGE, G. L. (1993). Characterisation of LTP induced by the activation of glutamate metabotropic receptors in area CA1 of the hippocampus. *Neuropharmacology* **32**, 1–9.

COLLINGRIDGE, G. L., KEHL, S. J. & MCLENNAN, H. (1983). Excitatory amino acids in synaptic transmission in the Schaffer collateral–commissural pathway of the rat hippocampus. *Journal of Physiology* **334**, 33–46.

CROUCHER, M. J., COLLINS, J. F. & MELDRUM, B. S. (1982). Anticonvulsant action of excitatory amino acid antagonists. *Science* **21**, 899–901.

DAVIES, J., FRANCIS, A. A., JONES, A. W. & WATKINS, J. C. (1981). 2-Amino-2-phosphonovalerate (2APV), a potent and selective antagonist of amino acid-induced and synaptic excitation. *Neuroscience Letters* **21**, 77–81.

DAVIES, S. N. & COLLINGRIDGE, G. L. (1989). Role of excitatory amino acid receptors in synaptic transmission in area CA1 of rat hippocampus. *Proceedings of the Royal Society* B **236**, 373–384.

FINE, A., AMOS, W. B., DURBIN, R. M. & MCNAUGHTON, P. A. (1988). Confocal microscopy: applications in neurobiology. *Trends in Neurosciences* **11**, 346–351.

FREY, U., KRUG, M., BRODEMANN, R., REYMANN, K. & MATTHIES, H. (1989). Long-term potentiation induced in dendrites separated from rat's CA1 pyramidal somata does not establish a late phase. *Neuroscience Letters* **97**, 135–139.

GIBB, A. J. & COLQUHOUN, D. (1991). Glutamate activation of a single NMDA receptor-channel produces a cluster of channel openings. *Proceedings of the Royal Society* B **243**, 39–45.

HARVEY, J. & COLLINGRIDGE, G. L. (1992). Thapsigargin blocks the induction of long-term potentiation in rat hippocampal slices. *Neuroscience Letters* **139**, 197–200.

HERNANDEZ-CRUZ, A., SALA, F. & ADAMS, P. R. (1990). Subcellular calcium transients visualised by confocal microscopy in a voltage clamped vertebrate neuron. *Science* **247**, 858–862.

HESTRIN, S., NICOLL, R. A., PERKEL, D. J. & SAH, P. (1990). Analysis of excitatory synaptic action in pyramidal cells using whole-cell recording from rat hippocampal slices. *Journal of Physiology* **422**, 203–225.

HOLLMANN, M., HARTLEY, M. & HEINEMANN, S. (1991). Ca^{2+} permeability of KA–AMPA-gated glutamate receptor channels depends on subunit composition. *Science* **252**, 851–853.

IINO, M., OZAWA, S. & TSUZUKI, K. (1990). Permeation of calcium through excitatory amino acid receptor channels in cultured rat hippocampal neurones. *Journal of Physiology* **424**, 151–165.

IRVING, A. J., COLLINGRIDGE, G. L. & SCHOFIELD, J. G. (1992). Interactions between Ca^{2+} mobilizing mechanisms in cultured rat cerebellar granule cells. *Journal of Physiology* **456**, 667–680.

KONNERTH, A., KELLER, B. U., BALLANYI, K. & YAARI, Y. (1990). Voltage sensitivity of NMDA-receptor-mediated postsynaptic currents. *Experimental Brain Research* **81**, 209–212.

KULLMANN, D. M., PERKEL, D. J., MANABE, T. & NICOLL, R. A. (1992). Ca^{2+} entry via postsynaptic voltage-sensitive Ca^{2+} channels can transiently potentiate excitatory synaptic transmission in the hippocampus. *Neuron* **9**, 1175–1183.

LYNCH, G., LARSON, J., KELSO, S., BARRIONUEVO, G. & SCHOTTLER, F. (1983). Intracellular injections of EGTA block induction of hippocampal long-term potentiation. *Nature* **305**, 719–721.

MALENKA, R. C., KAUER, J. A., PERKEL, D. J. & NICOLL, R. A. (1989). The impact of postsynaptic calcium on synaptic transmission–Its role in long-term potentiation. *Trends in Neurosciences* **12**, 444–450.

MALENKA, R. C., LANCASTER, B. & ZUCKER, R. S. (1992). Temporal limits on the rise in postsynaptic calcium required for the induction of long-term potentiation. *Neuron* **9**, 121–128.

MAYER, M. L., MACDERMOTT, A. B., WESTBROOK, G. L., SMITH, S. J. & BARKER, J. L. (1987). Agonist- and voltage-gated calcium entry in cultured mouse spinal cord neurons under voltage-clamp measured using arsenazo III. *Journal of Neuroscience* **7**, 3230–3244.

MODY, I., MACDONALD, J. F. & BAIMBRIDGE, K. G. (1988). Release of intracellular calcium following the activation of excitatory amino acid receptors in cultured hippocampal neurones. *Society for Neuroscience Abstracts* **14**, 94.

MONAGHAN, D. T. & COTMAN, C. W. (1986). Distribution of *N*-methyl-D-aspartate-sensitive L-[^{3}H]glutamate-binding sites in rat brain. *Journal of Neuroscience* **5**, 2909–2919.

MÜLLER, W. & CONNOR, J. A. (1991). Dendritic spines as individual neuronal compartments for synaptic Ca^{2+} responses. *Nature* **354**, 73–76.

OBENAUS, A., MODY, I. & BAIMBRIDGE, K. G. (1989). Dantrolene-Na (Dantrium) blocks induction of long-term potentiation in hippocampal slices. *Neuroscience Letters* **98**, 172–178.

RANDALL, A. D., BENKE, T. A., ANGELIDES, K., SCHOFIELD, J. G. & COLLINGRIDGE, G. L. (1990). A demonstration of NMDA receptor-mediated synaptic and single-channel currents from patch-clamped neurones in rat hippocampal slices. *Journal of Physiology* **425**, 18*P*.

RANDALL, A. D., SCHOFIELD, J. G. & COLLINGRIDGE, G. L. (1990). Whole-cell patch-clamp recordings of an NMDA receptor-mediated synaptic current in rat hippocampal slices. *Neuroscience Letters* **114**, 191–196.

REGEHR, W. G. & TANK, D. W. (1990). Postsynaptic NMDA receptor-mediated calcium accumulation in hippocampal CA1 pyramidal cell dendrites. *Nature* **345**, 807–810.

REGEHR, W. G. & TANK, D. W. (1992). Calcium concentration dynamics produced by synaptic activation of CA1 hippocampal pyramidal cells. *Journal of Neuroscience* **12**, 4202–4223.

SEGAL, M. & MANOR, D. (1992). Confocal microscopic imaging of $[Ca^{2+}]_i$ in cultured rat hippocampal neurons following exposure to *N*-methyl-D-aspartate. *Journal of Physiology* **448**, 655–676.

SIMON, R. P., SWAN, J. H., GRIFFITHS, T. & MELDRUM, B. S. (1984). Blockade of *N*-methyl-D-aspartate receptors may protect against ischemic damage in the brain. *Science* **226**, 850–852.

THASTRUP, O., CULLEN, P. J., DROBAK, B. K., HANLEY, M. R. & DANNIES, P. S. (1990). Thapsigargin, a tumor promoter, discharges intracellular calcium stores by specific inhibition of the endoplasmic reticulum Ca^{2+} ATPase. *Proceedings of the National Academy of Sciences of the USA* **87**, 2466–2470.

THAYER, S. A., HIRNING, L. D. & MILLER, R. J. (1988). The role of caffeine-sensitive calcium stores in the regulation of the intracellular free Ca concentration in rat sympathetic neurones *in vitro*. *Molecular Pharmacology* **34**, 664–673.

TSIEN, R. W. & TSIEN, R. Y. (1990). Calcium channels, stores, and oscillations. *Annual Review of Cell Biology* **6**, 715–760.

TSIEN, R. Y. (1988). Fluorescence measurement and photochemical manipulation of cytosolic free calcium. *Trends in Neurosciences* **11**, 419–424.

XU, Y. Z. & KRNJEVIC, K. (1990). Induction of long-term potentiation in isolated slices of Sprague–Dawley rat hippocampus is not blocked by dantrolene sodium. *Journal of Physiology* **426**, 50*P*.